Resistivity, magnetic-susceptibility, and specific-heat studies of $ErBa_2(Cu_{(1-x)}M_x)_3O_{7-y}$ [$(M=$Ni, Zn, Fe, Co, and Ga) and $x=0.005$]: The effect of site-dependent substitutional disorder

A. K. Bandyopadhyay, Deepak Varandani, E. Gmelin,* and A. V. Narlikar
National Physical Laboratory, New Delhi 110012, India
(Received 21 September 1993; revised manuscript received 1 February 1994)

We report here a systematic study of the resistivity, ac magnetic susceptibility, and specific-heat (C_p) anomalies in Er-1-2-3 systems for both the pure phase and when Cu is partly (0.5%) replaced by Ni, Zn, Fe, Co, and Ga. These substitutions are aimed at studying the role of site-dependent in-plane and out-of-plane disorder, in conjunction with fluctuation effects. Analysis of the results shows that, as compared to in-plane, the out-of-plane substitutions exhibit a domination of the fluctuation effect. This has been explained from the fact that the out-of-plane disorder substantially decouples the interlayer links between CuO_2 planes across the adjoining unit cells. This transforms the system to be more two dimensional, thereby enhancing the contribution of fluctuations.

I. INTRODUCTION

The fluctuation in the superconducting order parameter, just above T_c, has been known as an important effect responsible for a host of interesting phenomena, such as paraconductivity, field-induced broadening of R-T curves, precursor diamagnetic susceptibility, and excess specific heat, etc., as recently reviewed by various authors.[1,2] Although substitutional effects have been extensively studied in rare earth R-1-2-3 systems,[3] little attention has been paid to probing the fluctuation-induced effects in conjunction with chemical substitution in this system. It is well established[1,4] that, owing to their quasi-two-dimensional nature, coupled with their intrinsically very small coherence length (10 Å), fluctuation effects tend to become significantly more pronounced in high-T_c cuprates in comparison to the conventional low-T_c superconductors, which form three-dimensional systems with large coherence lengths of about 1000 Å. The low dimensionality of the cuprate superconductors essentially stems from their unusual layered structure, which comprises one or more planar CuO_2 layers with other cationic oxide (or pure cationic) layers intervening. With the exception of epitaxial thin films of these cuprates prepared under stringent conditions, the majority of samples[5] even in pure form generally exhibit significant resistive transition widths ΔT. The origin of the large ΔT is considered to be a manifestation of superconducting fluctuations in the form of excess conductivity at temperatures just above T_c.[6] Secondly, a comparatively broad specific-heat anomaly at T_c shown by high-T_c cuprates is also believed to be a direct consequence of fluctuations in the order parameter around T_c.[7,8]

In this paper we present a systematic study of the resistivity, magnetic susceptibility, and specific-heat anomaly in the Er-1-2-3 system for both the pure phase and when Cu is partly (0.5%) replaced by Ni, Zn, Fe, Co, and Ga. These substitutions are particularly interesting as the first two members tend to preferentially occupy[3] the Cu(2) site of the CuO_2 planes (to be referred to as in-plane disorder), while the latter three prefer the Cu(1) site of the CuO chains (i.e., out-of-plane disorder).

Purely from superconductivity considerations the main difference between these two substitutions is that the former interrupts CuO_2 planes where superconductivity is primarily supposed to reside, while the latter affects the chains and thereby influences the interlayer coupling between the successive stacks of CuO_2 planes of the neighboring unit cells along the c direction. The former has the effect of lowering the T_c while the latter tends to broaden the resistive transition.[6] The role of the interlayer coupling in broadening the resistive transition of the Bi-2122 system has been elaborated by Samanta *et al.*[9] A comparative study of the effects of the in-plane and out-of-plane substitutions in the Er-1-2-3 system on the resistivity, ac magnetic susceptibility, and specific-heat anomaly should provide a useful insight into the possible role of fluctuations associated with the site-dependent disorder in the Er-1-2-3 system.

II. EXPERIMENTAL DETAILS

The bulk polycrystalline samples of nominal composition $ErBa_2(Cu_{(1-x)}M_x)_3O_{7-y}$ ($M=$Ni, Zn, Fe, Co, and Ga and $x=0.005$) were prepared by solid state reaction using ingredients of purity 99.99%. The different samples (pure, Cu/Ni, Cu/Zn, Cu/Fe, Cu/Co, and Cu/Ga) are designated as (1) Er-1-2-3 (pure), (2) Er-1-2-3 (Ni), (3) Er-1-2-3 (Zn), (4) Er-1-2-3 (Fe), (5) Er-1-2-3 (Co), and (6) Er-1-2-3 (Ga).

The synthesis procedure has already been discussed elaborately by Narlikar, Agarwal, and Rao.[3] In brief, single-phase samples were prepared by grinding the corresponding oxides and carbonates in the appropriate stoichiometric ratios, and calcining them three times at 900, 910, and 920 °C, respectively. Each calcination started with thorough grinding and pelletization of the samples, followed by calcination at that temperature for about 15–20 h and, subsequently, the samples were

quenched to room temperature. The final reaction was carried out in oxygen, first at 940 °C for about 15 h and then the furnace was cooled down to 600 °C. At that temperature and maintaining the same oxygen pressure, the samples were held for another 6 h, followed by furnace cooling down to room temperature. Because of simultaneous oxygen annealing of all these samples in the same batch, the oxygen content of all these samples is assumed to be nearly identical.

X-ray diffraction (XRD) of the samples for phase purity was carried out using a Siemens D-500 diffractometer with Cu $K\alpha$ radiation. The scanning electron micrographs (SEM) for different specimens were recorded in secondary-electron-emission mode with a 0° tilt using a JOEL JSM 35 CF instrument. The conventional four-probe technique was used for studying the resistive transition of the samples.

The ac magnetic susceptibility was measured by a Lakeshore 7000 susceptometer. All the samples were cooled in a low field of 0.025 Oe (rms), frequency 111.1 Hz, through the transition temperature (T_c), and χ' and χ'' were measured while warming up slowly. In order to calculate the demagnetization factor, the samples are cut in the same geometric dimension and are placed inside a Teflon capsule. The susceptometer was calibrated from time to time using a standard sample provided by the manufacturer.

The specific heat was measured by a fully automated quasiadiabatic calorimeter, where the instrument control and data acquisition were carried out through a Hewlett-Packard (HP) 9332 model computer.[10] The sample holder was a sapphire block (diameter is 8 mm), PTR 100 was used as thermometer, and the heating element was made from Ni-Cr film deposited on a thin sapphire plate. Silicon diodes were used to monitor and control the temperature of the thermal shield through a temperature controller (Lakeshore 91C). The temperature drift curve in the post-heating period was measured with the exponential function as described by Ota and Gmelin.[11] The specific heat of the sample was obtained by subtracting the heat capacity of the addenda consisting of a sapphire block, a heating element, and Apiezon N grease, etc.; OFHC (oxygen-free high-conductivity) copper was used for calibration, and it turns out that the absolute error in the specific-heat measurement is estimated to be less than 1%. The details of the measuring setup and the calibration procedure of the instrument will be published elsewhere.[12]

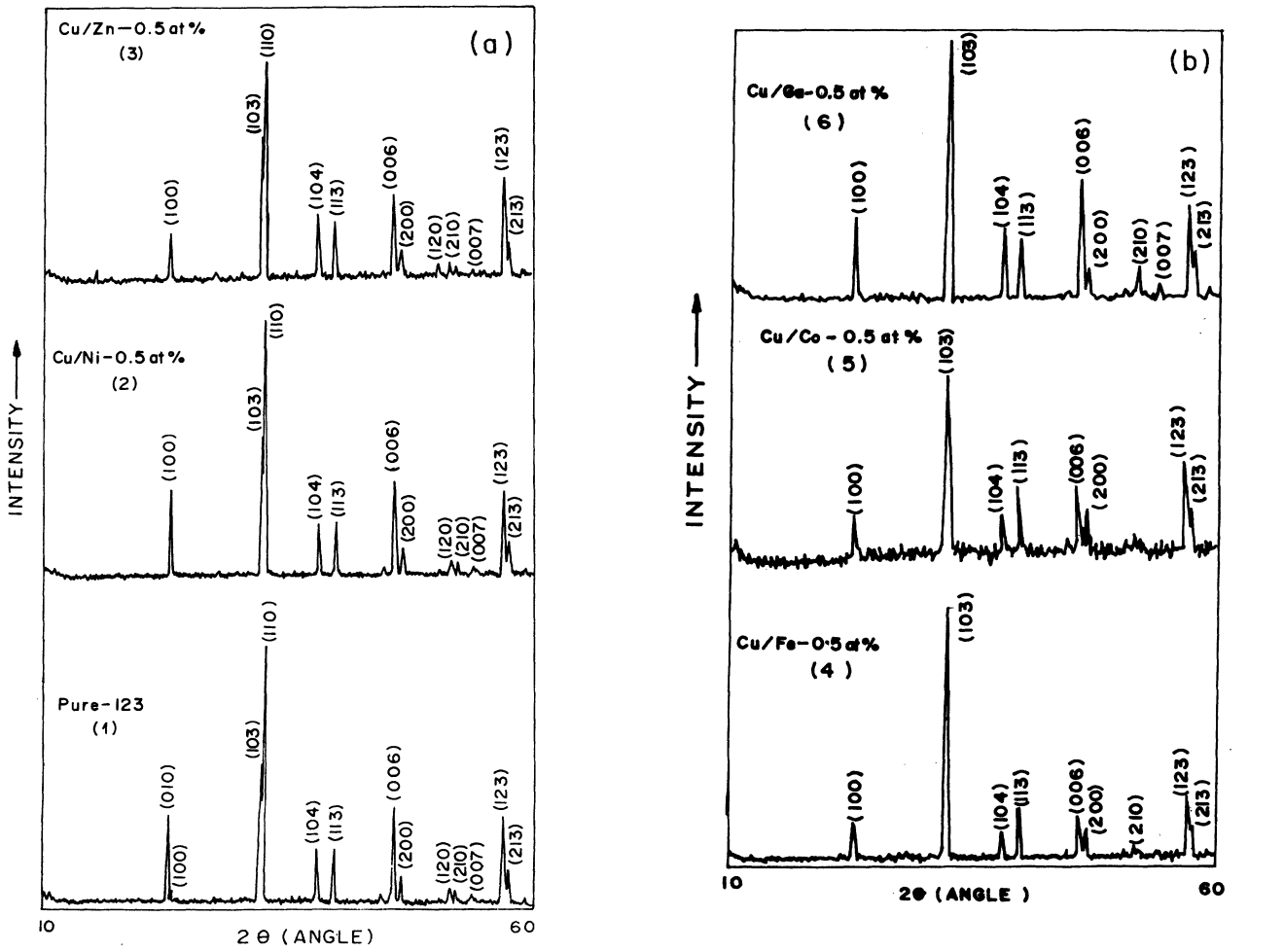

FIG. 1. XRD pattern of (a) (1) Er-1-2-3 (pure), (2) Er-1-2-3 (Ni), and (3) Er-1-2-3 (Zn); (b) (4) Er-1-2-3 (Fe), (5) Er-1-2-3 (Co), and (6) Er-1-2-3 (Ga).

TABLE I. Lattice parameters of the six samples

Sample	a (Å)	b	c
Er-1-2-3 (pure)	3.82	3.89	11.63
Er-1-2-3 (Ni)	3.82	3.89	11.62
Er-1-2-3 (Zn)	3.82	3.89	11.63
Er-1-2-3 (Fe)	3.83	3.86	11.64
Er-1-2-3 (Co)	3.83	3.87	11.63
Er-1-2-3 (Ga)	3.84	3.86	11.64

III. RESULTS

A. XRD

Figure 1(a) shows the XRD pattern of the samples Er-1-2-3 (pure), Er-1-2-3 (Ni), and Er-1-2-3 (Zn). It is clear that all the important and major peaks, corresponding to the (110) and (103), (104), (113), (123) and (213), etc., reflections for the orthorhombic structure are found in these samples. The expected orthorhombic splitting associated with (110) and (103) as well as (123) and (213) reflections can clearly be observed in all three samples. This indicates that the orthorhombic distortion as has been reported in Er-1-2-3 (pure),[13] is clearly observable in Er-1-2-3 (Ni) and Er-1-2-3 (Zn) samples. Figure 1(b) shows the XRD patterns of the samples Er-1-2-3 (Fe), Er-1-2-3 (Co), and Er-1-2-3 (Ga). Here also all the prominent peaks corresponding to (103), (104), (113), (123) and (213), etc., reflections of the orthorhombic structure are present. Therefore, the substitution process in Er-1-2-3 (Ni) and Er-1-2-3 (Zn) is not significantly different from that in Er-1-2-3 (Fe), Er-1-2-3 (Co), and Er-1-2-3 (Ga). Furthermore, there are no additional unidentified peaks. This suggests the upper limit of 1–3 % for the level of any impurity phase, and there is really no reason to believe that the impurity phase is particularly more in the latter three substituted samples.

The lattice parameters for these six samples (shown in Table I) are obtained by our optimization program taking into account all of the peaks. The observed d values are compared with the calculated d values and the difference $(d_{obs}-d_{cal})$ occurs in the third decimal place. Within this level of measuring accuracy, clearly the material remains orthorhombic for all substitutions, but with less orthorhombicity for the Fe-, Co-, and Ga-substituted samples.

B. SEM

SEM studies reveal that there is a homogeneous and uniform distribution of grains with sizes ranging between 2 and 6 μm for all the samples. Typical SEM micrographs for pure and Co-substituted samples are shown in Figs. 2 and 3.

C. Resistivity

Figure 4 shows the variation of resistivity with temperature in the range 77–290 K for all six samples and the inset shows T_c(onset) and $T_c(R=0)$. $T_c(R=0)$ is 92.5, 89.1, 86.2, 88.5, 89.9, and 89.5 K for the samples Er-1-2-3 (pure), Er-1-2-3 (Ni), Er-1-2-3 (Zn), Er-1-2-3 (Fe), Er-1-2-3 (Co), and Er-1-2-3 (Ga), respectively. T_c(onset) can be seen for all samples in the inset of Fig. 4 to decrease with different substitutions also. Even at this low doping level, $T_c(R=0)$ decreases with doping and the maximum depression (6 K) has been observed for Er-1-2-3 (Zn). Figure 5 shows the temperature derivative of normalized resistivity $(d\rho_N/dT)$ as a function of temperature for the samples Er-1-2-3 (pure), Er-1-2-3 (Ni), Er-1-2-3 (Zn), Er-1-2-3 (Fe), Er-1-2-3 (Co), and Er-1-2-3 (Ga), respectively [normalization was carried out with reference to Er-1-2-3 (pure)]. These figures reveal that the width of the transition $(\Delta T)_R$ for the former three samples is smaller than that for the latter three samples. As mentioned earlier, all the samples have been prepared under identical conditions, so that the $(\Delta T)_R$ in the latter three substituted samples is thought to be attributable to the intrinsic properties of the superconducting phase.

FIG. 2. SEM micrograph of Er-1-2-3 (pure).

FIG. 3. SEM micrograph of Er-1-2-3 (Co).

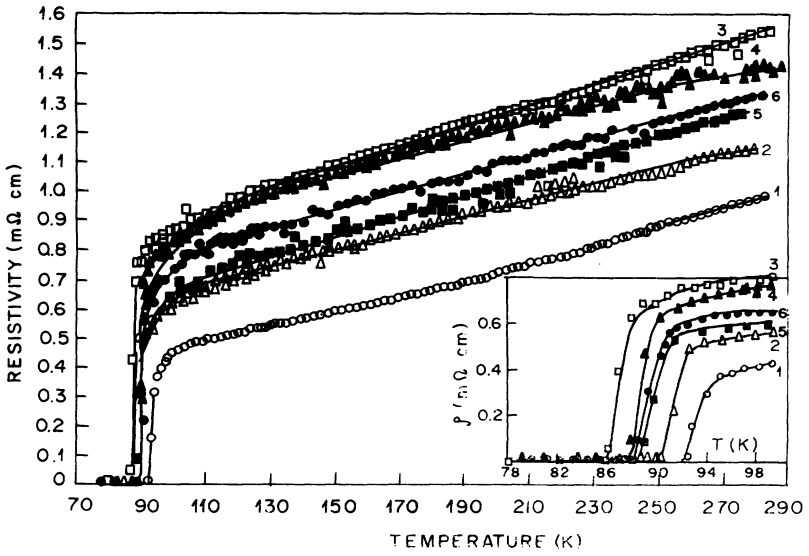

FIG. 4. Resistivity (ρ) vs temperature (T) curves for (1) Er-1-2-3 (pure), (2) Er-1-2-3 (Ni), (3) Er-1-2-3 (Zn), (4) Er-1-2-3 (Fe), (5) Er-1-2-3 (Co), Er-1-2-3 (Ga); and the inset shows ρ-T curves for all the samples close to T_c.

D. ac susceptibility

Figure 6 shows the results of susceptibility ($\chi=\chi'-i\chi''$) measurements in the temperature range 77–130 K for all the samples. From χ' data, the onset of the superconducting transition is 90.5, 89.5, 86, 90, 88.5, and 89.6 K for the samples Er-1-2-3 (pure), Er-1-2-3 (Ni), Er-1-2-3 (Zn), Er-1-2-3 (Fe), Er-1-2-3 (Co), and Er-1-2-3 (Ga), respectively. As previously reported[14] the susceptibility and magnetization data are difficult to interpret in terms of the percentage of full diamagnetism as the field-cooled values (Meissner fraction) are dependent on other factors, such as external field, sample size, and perfection, and can bear little relation to the proportion of the superconducting phase present in the sample. Moreover, it may also be possible that the relative change in the diamagnetic signal could also reflect an improvement in the superconductivity at the grain boundaries or a better connection of superconducting paths in the sample. Furthermore, Hein[15] and Goldfarb, Lelenthal, and Thompson[16] have pointed out that ceramic samples must be pulverized, the intergranular coupling must be depressed, and/or the χ' value should be taken well below the intrinsic T_c; even then, the superconducting volume fraction is only an estimate. However, as mentioned,[17] the measurements were carried out under field-cooled and identical conditions on different samples; the diamagnetic amplitude at a particular temperature can be compared in the first approximation. The lower inset of Fig. 6 shows the size of the χ' signals at 77 K normalized to that for Er-1-2-3 (pure). It is clear that the diamagnetic amplitude at 77 K for the samples Er-1-2-3 (Ni) and Er-1-2-3 (Zn) is nearly the same; however, for the samples Er-1-2-3 (Fe), Er-1-2-3 (Co), and Er-1-2-3 (Ga), it is reduced.

The peak χ'', which is also linked with the diamagnetic transition and is influenced by the Josephson-like coupling between the grains, is shown in the upper inset of Fig. 6 [normalized with reference to χ'' of Er-1-2-3 (pure)]. It may be mentioned here[3] that both these χ' and χ'' values are very sensitive to the intragranular and in-

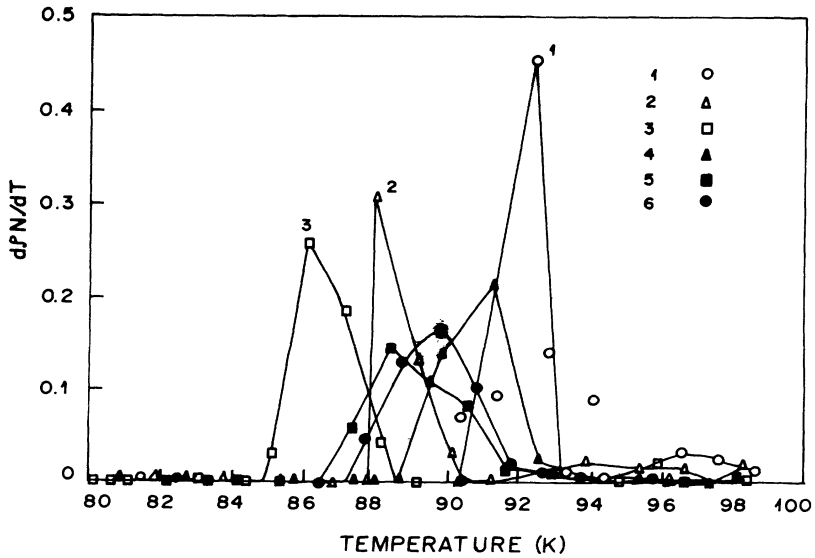

FIG. 5. ($d\rho_N/dT$) vs T for (1) Er-1-2-3 (pure), (2) Er-1-2-3 (Ni), (3) Er-1-2-3 (Zn), (4) Er-1-2-3 (Fe), (5) Er-1-2-3 (Co), and (6) Er-1-2-3 (Ga) [ρ_N is the normalized resistivity].

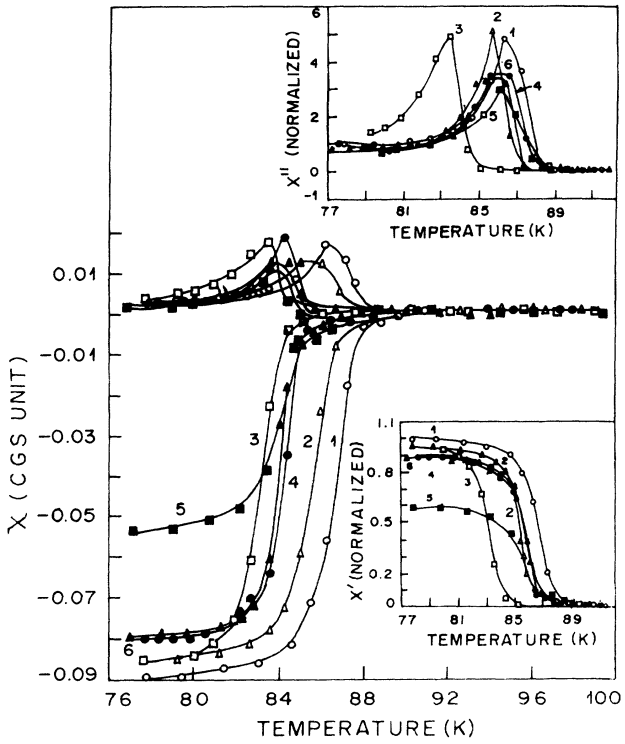

FIG. 6. ac susceptibility ($\chi=\chi'-i\chi''$) vs temperature (T) curves for (1) Er-1-2-3 (pure), (2) Er-1-2-3 (Ni), (3) Er-1-2-3 (Zn), (4) Er-1-2-3 (Fe), (5) Er-1-2-3 (Co), and (6) Er-1-2-3 (Ga). Lower inset, χ' (normalized) vs T curves; upper inset, χ'' (normalized) vs T curves.

tergranular superconductivity. The fact that the behavior of χ'' for all the substituted samples is essentially analogous indicates that there is no reason to believe that weak-link effects are more dominant for one set of substitutions than the other.

Finally, all the samples were cut to the same dimension and have undergone the same sintering conditions (method of calcinations, oxygen flow, furnace temperatures, pressure exerted during the formation of the pellet, etc.). Thus, it is assumed that the demagnetization factors are similarly corrected. Therefore, one can compare the width of the superconducting transition as observed in χ' [$(\Delta T)\chi'$] in these samples. Figure 7 shows $d\chi'/dT$ as a function of temperature for Er-1-2-3 (pure), Er-1-2-3 (Ni), Er-1-2-3 (Zn), Er-1-2-3 (Fe), Er-1-2-3 (Co), and Er-1-2-3 (Ga). Like $(\Delta T)_R$, the width of the transition of the susceptibility plot [$(\Delta T)\chi'$] for Ni- and Zn-substituted samples is more or less the same as for the pure sample; however, it is comparatively larger for the Fe-, Co-, and Ga-substituted samples.

E. Specific heat

Although C_p was studied in the temperature range 300–77 K, as reported earlier,[18] we concentrate on the data at temperatures close to T_c. Figure 8 shows distinct and clear C_p anomalies at 90, 88, and 86 K, respectively, for the samples Er-1-2-3 (pure), Er-1-2-3 (Ni), and Er-1-2-3 (Zn). The inset of Fig. 8 shows the plot of C_p/T against temperature for the same samples. Figure 9 shows the specific-heat data of the samples Er-1-2-3 (Fe), Er-1-2-3 (Co), and Er-1-2-3 (Ga), and the inset depicts the plot of C_p/T with temperature. The specific-heat anomaly is also seen for these samples but it is relatively broad and smeared. The specific-heat jump turns out to be within 4.5 J/mol K for the pure, Ni-, and Zn-substituted samples, while for the samples with Fe, Co, and Ga, it is less than 3 J/mol K. The estimated $\Delta C_p/T_c$ for these samples is 20–48 mJ/mol K^2, which agrees well with the published data.[13,18]

The characteristic parameters, like the Sommerfeld constant (ν) or Debye temperature (Θ_D), are difficult to estimate in these oxide superconductors because the electronic contribution of specific heat in the specific-heat

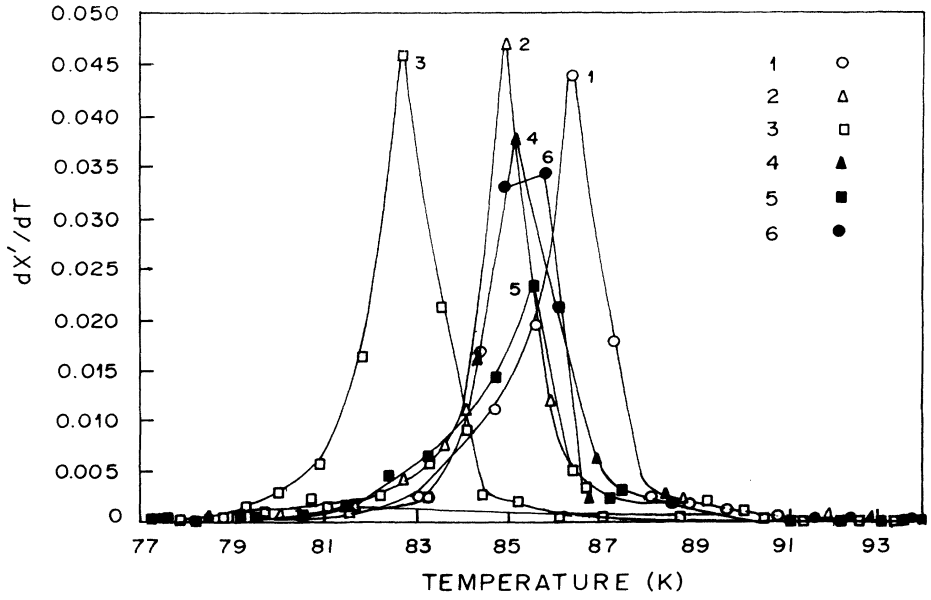

FIG. 7. ($d\chi'/dT$) vs T for (1) Er-1-2-3 (pure), (2) Er-1-2-3 (Ni), (3) Er-1-2-3 (Zn), (4) Er-1-2-3 (Fe), (5) Er-1-2-3 (Co), and (6) Er-1-2-3 (Ga).

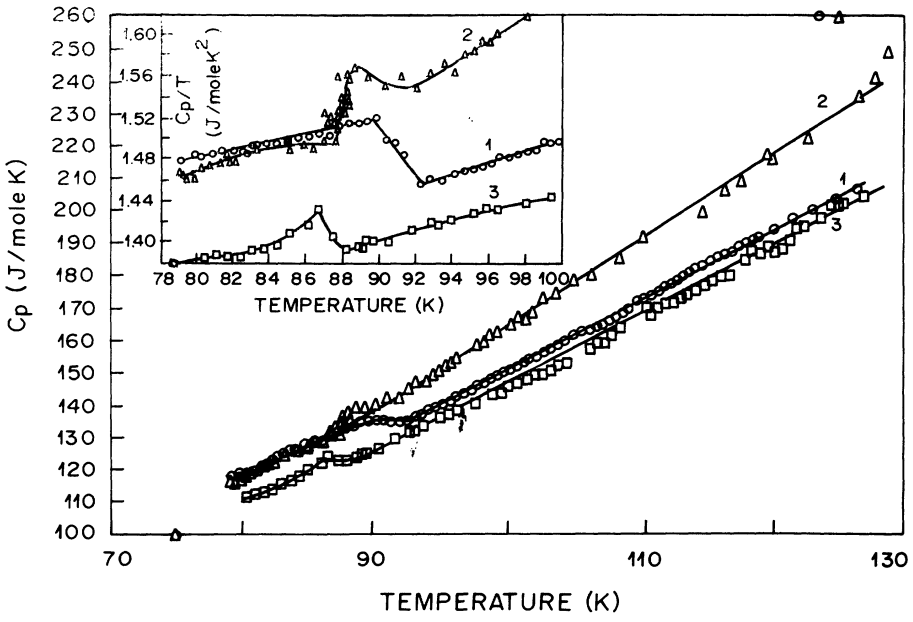

FIG. 8. Molar specific heat (C_p) vs temperature (T) curves for (1) Er-1-2-3 (pure), (2) Er-1-2-3 (Ni), and (3) Er-1-2-3 (Zn); the inset shows C_p/T vs T for these samples.

anomaly is strongly affected by the phononic contribution.[10] However, in order to indicate the possible trend in the nature of the coupling, the Sommerfeld constant (ν) was estimated as discussed earlier.[19] After correcting the temperature-independent susceptibility for diamagnetic core and Landau contributions in the usual way for the pure sample, we obtain ν as 40 mJ/mol K^2. The reported values of ν in these systems lie in the range 20–50 mJ/mol K^2 and our rough value falls within this region.[13] Similarly, the Debye temperature is calculated from the specific-heat data at various temperatures, using the theoretical Debye function on the assumption that the three-dimensional Debye model is valid in this system. An iterative method has been developed to obtain the best-fitted value. The Debye temperatures obtained are found to be temperature dependent, and the average value of the Debye temperature around the transition temperature is found to be 440 K, which agrees well with the earlier value.[13]

IV. DISCUSSION

The results from these combinations of experiments indicate two distinct types of behavior.

(i) When the divalent Ni and Zn were substituted, (a) both the $(\Delta T)_R$ and $(\Delta T)_{\chi'}$ are comparable to those for the pure sample, (b) the relative size of the χ' signal at 77 K is comparable to that of the pure sample, and (c) there is a clear specific-heat anomaly.

(ii) When trivalent Fe, Co, and Ga were substituted, (a)

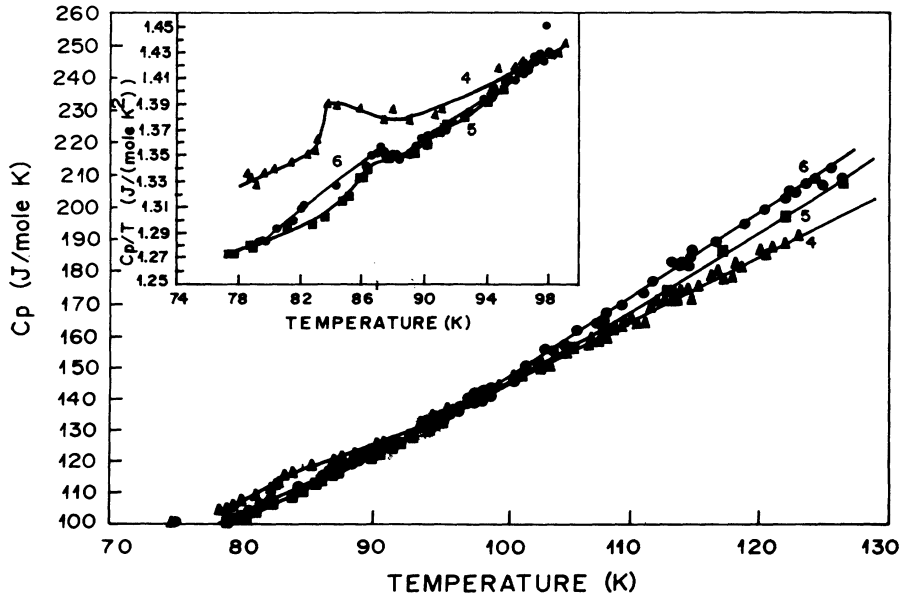

FIG. 9. Molar specific heat (C_p) vs temperature (T) curves for (4) Er-1-2-3 (Fe), (5) Er-1-2-3 (Co) and (6) Er-1-2-3 (Ga); the inset shows C_p/T vs T for these samples.

both $(\Delta T)_R$ and $(\Delta T)_{\chi'}$ are comparatively large, (b) the relative size of the χ' signal at 77 K is reduced for Fe- and Ga-substituted samples (more so for Co-substituted samples), and (c) there is a broad specific-heat anomaly.

It may be emphasized here that, as discussed, XRD and SEM studies for the above series of samples have given no indication of any macroscopic inhomogeneities in either in-plane or out-of-plane substitution. Thus the above results may be ascribed primarily to the substitutions. In this context, it is interesting to mention that experiments on bulk Y-124 samples had showed the transition at T_c to be noticeably broader for Fe, Co, and Ga substitution than for Ni and Zn substitution.[20]

In order to understand the situation described above, we first analyze the resistivity data of all the samples in the mean-field theory (MFT) to determine the excess conductivity due to fluctuation. The total conductivity[1,6] is decomposed into a linear background resistivity which is a straight-line fit $[\rho^B(T)=\rho_0+BT]$, plus a part due to fluctuations in the thermodynamic Ginzburg-Landau temperature which is shown for a pure sample in Fig. 10. The fitted values of ρ_0 and B turn out to be 0.182 m Ω cm and 2.716 μΩ cm/K. The excess conductivity $(\Delta\sigma)$ which is $1/\rho(T)-1/\rho^B(T)$, can be written in the framework of a simple Aslamazov-Larkin (AL) fit as

$$\Delta\sigma=(e^2/16ht)[(T-T_c)/T_c]^{-d}, \quad (1)$$

where t is the thickness and d is the dimensionality of the sample. We have plotted $\ln[(T-T_c)/T_c]$ vs $\ln(\Delta\sigma)$ which is shown in the inset of Fig. 10. We do not find a single linear region which seems to indicate that there is no single power-law dependence of the fluctuations. However, when the fit is carried out within 5 K of T_c, d turn sout to be 1.0±0.1 which corresponds to two-dimensional (2D) fluctuations. Similarly, for the other samples Er-1-2-3 (Ni), Er-1-2-3 (Zn), Er-1-2-3 (Fe), Er-1-2-3 (Co), and Er-1-2-3 (Ga), the fitted background contributions of ρ_0 and B were found to be 0.367, 0.606, 0.466,

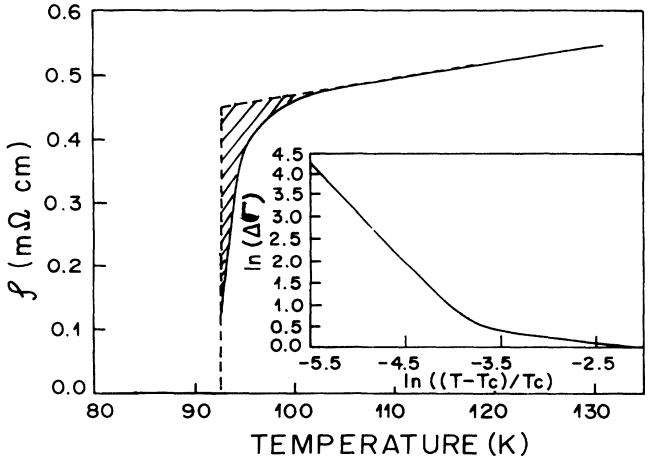

FIG. 10. ρ vs temperature for Er-1-2-3 (pure); the dotted line shows the fitting of the data with $\rho^B(T)=\rho_0+BT$ and the hatched portion shows $\Delta\sigma(T)$; the inset shows $\ln(\Delta\sigma)$ vs $\ln[(T-T_c)/T_c]$.

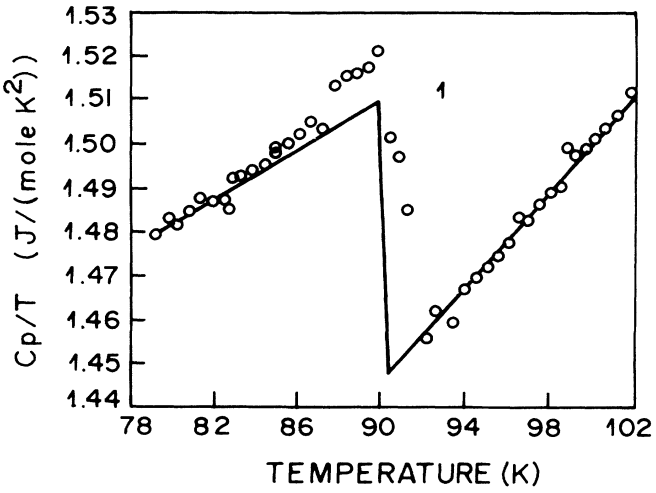

FIG. 11. C_p/T vs temperature for (1) Er-1-2-3 (pure); the continuous line shows the fitting of the data with $C_p^B/T=a_0+bT$ both above and below T_c.

0.533, and 0.344 m Ω cm and 3.150, 3.008, 3.106, 2.974, and 3.102 μΩ cm/K, respectively. Upon plotting $\ln[(T-T_c)/T_c]$ vs $\ln(\Delta\sigma)$, the d values obtained [from Eq. (1)] are 1.120, 1.043, 1.020, 1.033, and 1.102, respectively. These show that the 2D AL fit works well in all our samples.

We have analyzed also the C_p data of all samples in the MFT to determine the excess C_p due to fluctuations. Following a similar approach as for the resistivity, a smooth background of phononic contribution $C_p^B/T=a_0+bT$ is

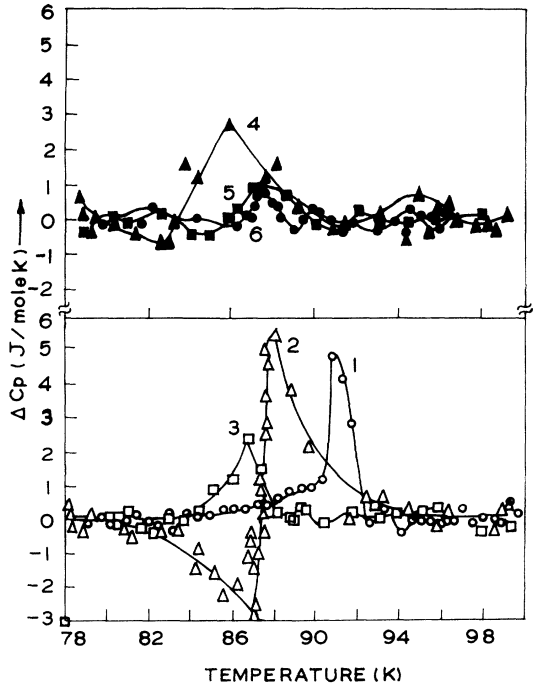

FIG. 12. Excess specific heat (ΔC_p) vs temperature for (1) Er-1-2-3 (pure), (2) Er-1-2-3 (Ni), (3) Er-1-2-3 (Zn), (4) Er-1-2-3 (Fe), (5) Er-1-2-3 (Co), and (6) Er-1-2-3 (Ga).

constructed both above and below T_c, and this is shown in Fig. 11 for the pure sample. The excess specific heat (ΔC_p), which is essentially ($C_p - C_p^B$), is shown for all the samples in Fig. 12. A plot obtained of $\ln(\Delta C_p)$ and $\ln[(T-T_c)/T_c]$ (not shown) revealed that there is no single linear region, indicating the absence of any single power-law dependence of the fluctuations. However, when the fit is carried out in the region within 5 K of T_c, the slope of the linear region turns out to within 1.0 ± 0.1, which is indicative of the two-dimensional nature of the fluctuation. Furthermore, we see that the observed C_p anomaly for Ni- and Zn-substituted samples is as distinct as that for the pure sample. On the other hand, the C_p anomaly observed for Fe-, Co-, and Ga-substituted samples is significantly broadened, illustrating that the effect of fluctuations in Fe-, Co-, and Ga-substituted samples is comparatively much larger than in Ni- and Zn-substituted samples. This is again indicative of a more pronounced fluctuation effect occurring when Fe, Co, and Ga are incorporated at the Cu(1) site.

These findings, we suggest, are the direct manifestation of in-plane and out-of-plane disorder which the above substitutions create in the 1-2-3 structure. Zn and Ni, as they occupy CuO_2 planes,[3] mainly contribute to a decrease in T_c, while they have little influence on the interlayer coupling between CuO_2 layers across the neighboring unit cells. On the other hand, Fe, Co, and Ga, preferring to substitute at the chain Cu(1) site,[3] create out-of-plane disorder between the CuO_2 layers of the adjoining unit cells and thereby weaken the coupling between them in the c direction, where the range of coherence is already low. In effect, this possibly results in transforming the system more toward two dimensions, leading to increased fluctuation effects, as observed in the specific-heat data of the present study.

ACKNOWLEDGMENTS

The authors thank Professor S. K. Joshi of CSIR for his keen interest and V. P. S. Awana, V. N. Morthy, B. V. Kumarswamy, and V. S. Yadav for their experimental help. One of us (E.G.) thanks CSIR and DAAD for providing the opportunity of visiting NPL for research collaboration.

*Permanent address: Max-Planck-Institut für Festkörperforschung, Heisenbergstrasse 1, D-70506, Stuttgart, Germany.

[1]Y. Iye, in *Studies of High Temperature Superconductors*, edited by A. Narlikar (Nova, New York, 1989), Vol. 1, p. 166.

[2]M. Akinaga, in *Studies of High Temperature Superconductors* (Ref. 1), Vol. 8, p. 297.

[3]A. V. Narlikar, S. K. Agarwal, and C. V. N. Rao, in *Studies of High Temperature Superconductors* (Ref. 1), Vol. 1, p. 341.

[4]W. J. Skocpol and M. Tinkham, Rep. Prog. Phys. **38**, 1049 (1975).

[5]S. B. Ogale, R. D. Vispule, and S. M. Kanetkar, Indian J. Pure Appl. Phys. **30**, 666 (1992).

[6]A. V. Narlikar, R. Lal, and E. Gmelin (unpublished).

[7]D. Sanchez, A. Junod, J.-Y. Genoud, T. Graf, and J. Muller, Physica C **200**, 1 (1992).

[8]S. E. Inderhees, M. B. Salamon, N. Goldenfeld, J. P. Rice, B. G. Pazol, D. M. Ginsberg, J. Z. Liu, and G. W. Crabtree, Phys. Rev. Lett. **60**, 1178 (1988).

[9]S. B. Samanta, P. K. Dutta, V. P. S. Awana, E. Gmelin, and A. V. Narlikar, Physica C **178**, 171 (1991).

[10]E. Gmelin, in *Studies of High-Temperature Superconductors* (Ref. 1), Vol. 2, p. 95.

[11]S. B. Ota and E. Gmelin, Meas. Sci. Technol. **3**, 1047 (1992).

[12]A. K. Bandyopadhyay, E. Gmelin, V. S. Yadav, and A. V. Narlikar (unpublished).

[13]D. R. Harshman and A. P. Mills, Jr., Phys. Rev. B **45**, 10 684 (1992).

[14]A. Sumiyama, H. Endo, J. Tsuchiya, N. Kijima, M. Mizuno, and Y. Oguri, Jpn. J. Appl. Phys. **28**, L373 (1989).

[15]R. A. Hein, Phys. Rev. B **33**, 7539 (1986).

[16]R. B. Goldfarb, M. Lelental, and C. A. Thompson, *Magnetic Susceptibility of Superconductors and Other Spin Systems* (Plenum, New York, 1991), pp. 49–80.

[17]A. K. Bandyopadhyay, E. Gmelin, B. V. Kumaraswamy, V. P. S. Awana, Deepak Varandani, Nirupa Sen, and A. V. Narlikar, Phys. Rev. B **48**, 6470 (1993).

[18]A. K. Bandyopadhyay, P. Maruthikumar, G. L. Bhalla, S. K. Agarwal, and A. V. Narlikar, Physica C **165**, 29 (1990).

[19]Y. Gao, E. Crow, G. H. Myer, P. Schlottmann, J. Schwegler, and N. D. Spencer, Physica C **165**, 340 (1990).

[20]S. P. Pandey, M. S. Hegde, B. V. Kumaraswamy, and A. V. Narlikar, Physica C **206**, 207 (1993).

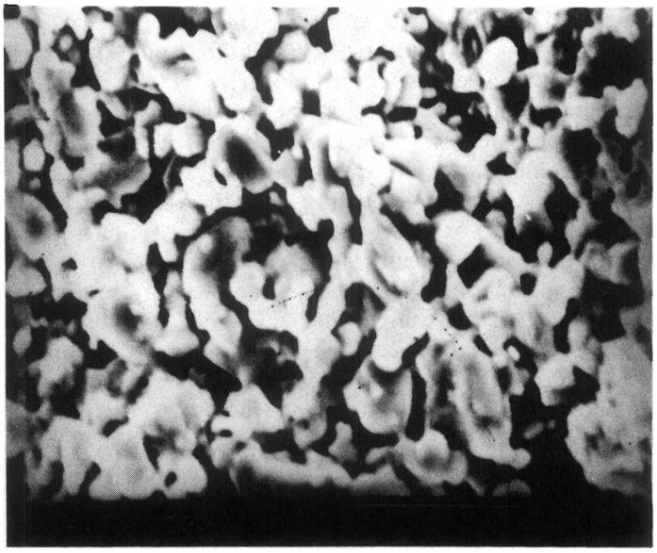

FIG. 2. SEM micrograph of Er-1-2-3 (pure).

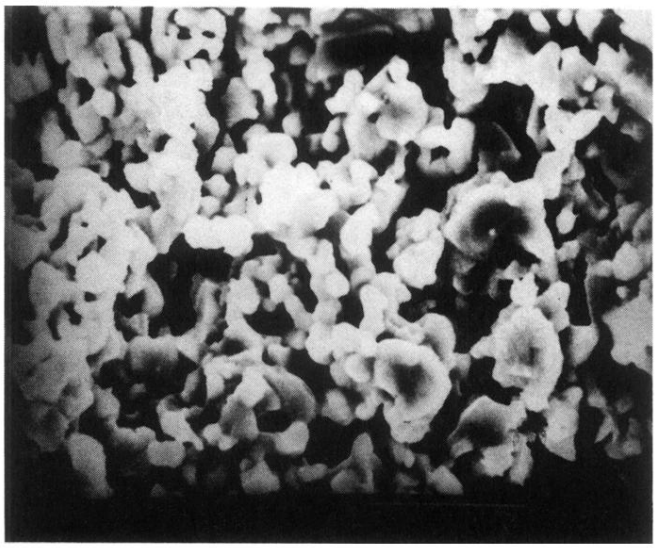

FIG. 3. SEM micrograph of Er-1-2-3 (Co).